

# A Massively Parallel Interior-Point-Method for Arrowhead Linear Programs

Nils-Christian Kempke\*, Daniel Rehfeldt†

Thorsten Koch‡

July 26, 2019

## Abstract

In practice, non-specialized interior point algorithms often cannot utilize the massively parallel compute resources offered by modern many- and multi-core compute platforms. However, efficient distributed solution techniques are required, especially for large-scale linear programs. This article describes a new decomposition technique for systems of linear equations implemented in the parallel interior-point solver PIPS-IPM++. The algorithm exploits a matrix structure commonly found in optimization problems: a doubly-bordered block-diagonal or arrowhead structure. This structure is preserved in the linear KKT systems solved during each iteration of the interior-point method. We present a hierarchical Schur complement decomposition that distributes and solves the linear optimization problem; it is designed for high-performance architectures and scales well with the availability of additional computing resources. The decomposition approach uses the border constraints' locality to decouple the factorization process. Our approach is motivated by large-scale unit-commitment problems. We demonstrate the performance of our method on a set of mid-to large-scale instances, some of which have more than  $10^9$  nonzeros in their constraint matrix.

## 1 Introduction

As of today, many real-world energy system models (ESMs) that describe energy systems are mathematically modeled and solved as linear problems (LPs). Since energy sources such as wind, solar, and hydroelectric are not readily available everywhere and their energy production is often much less centralized, energy systems and the corresponding ESMs become larger and more connected. This translates to the requirements imposed on mathematical solution software. The wish to solve bigger models, whether in the spatial, temporal, or technological dimension, is an ever-present motivation in energy system modeling.

While significant progress has been made in the last years for solving LPs [5, 23], even today's best commercial solvers often cannot find solutions for mid-

---

\*  0000-0003-4492-9818

†  0000-0002-2877-074X

‡  0000-0002-1967-0077

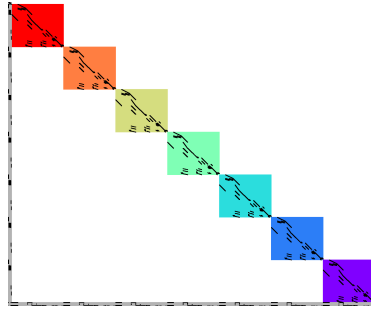


Figure 1: Constraint matrix with doubly-bordered block diagonal structure of ESMs.

to large-scale ESMs within a reasonable time. Fortunately, parallel computing hardware is becoming more available, and its cost is continuously decreasing; one way forward is to develop and implement highly parallel, specialized algorithms. While general LP solution techniques often scale poorly on such hardware, specialized solutions promise to overcome scaling issues and push back the current limits by exploiting the massive power of modern high-performance computing (HPC). A characteristic structure of the LPs that model linear ESMs is the arrowhead or doubly-bordered block-diagonal form depicted in fig. 1. Arrowhead LPs (AHLPs) exhibit linking variables and constraints. Linking variables connect two or more diagonal blocks vertically, and linking constraints connect two or more blocks horizontally. Notably, this structure is not restricted to ESMs but can be found in time-expanded spatial and technological networks and the solution strategies presented in this article apply to a broad class of models. AHLPs also included primal block angular and dual block angular problems and, as such, multistage or staircase problems, generalized bounds, and multi-commodity flow problems. There has been much research activity in decomposing AHLPs and their sub-problems [10, 26, 33, 35]. In particular, the class of primal-block angular LPs has attracted considerable interest in the past since it forms the basis for two-stage stochastic optimization problems for which powerful parallel solvers exist: BlockIp [11], OOPS [24, 25], and PIPS-IPM [40].

In earlier work [42], we extended the solver PIPS-IPM (based on OOPS) from the primal block angular problems class to AHLPs. Although the resulting solver PIPS-IPM++ could solve large-scale instances, one of its main bottlenecks was the assembly and solution of the so-called Schur complement. The size of the Schur complement is directly related to the amount of linking structure present in the AHLP. Since factorizing and solving with the Schur complement were done sequentially or in shared memory parallel, this posed a bottleneck for the algorithm and imposed a limit on the scalability of PIPS-IPM++.

The main contribution of this article is the description and implementation of a novel approach within PIPS-IPM++, called *hierarchical Schur complement approach* (HSCA) based on the observation that many linking constraints in the problem only link a few (often two) consecutive blocks. Therefore, the Schur complement can be distributed and split into multiple smaller ones, enabling us to solve instances with up to 1.7 million linking constraints and variables. For the computational evaluation of HSCA, we rely on two different sources of ESMs. First, we tested PIPS-IPM++ on the SIMPLE instances developed during

the research projects BEAM-ME<sup>1</sup> and UNSEEN<sup>2</sup>, see [42, 43]. These simplified models aim to capture the general features of ESMs accurately. The number and size of the diagonal blocks can be controlled precisely without incurring additional modeling overhead. Second, we considered a variant of the REMix models [21] called REMix-MISO. REMix is an ESM modeling framework developed at the German aerospace center<sup>3</sup>. During the BEAM-ME and UNSEEN projects, these models were extended and formed the motivation for the development of PIPS-IPM++. For more details on the models, the reader is referred to [9, 20].

## 2 Interior-point Methods for Linear Programming

The main two methods for solving general LPs are the simplex algorithm [12] and interior-point methods [46]. Often, IPMs are more successful on large problems and offer more potential for parallelization. This success can be explained by the fact that the IPM’s main computational effort is matrix factorization, and the amount of factorizations required grows relatively slowly with the problem size [41]. Many algorithms fall into the notion of IPMs, see [39, 44, 46]. In this work, we use an infeasible primal-dual IPM similar to the ones described in [18, 37] using Mehrotra’s predictor corrector scheme extended by Gondzio corrector steps [14]. In the following, we omit many details on the IPM method, and instead focus on the main feature of HSCA: the hierarchical decomposition of AHLPs. Details of the actual IPM can be found in [25, 34, 40] and the references mentioned before.

### 2.1 Notation

We often write  $0$  for a zero-vector or matrix; we will explain further when the context requires it. As is often the case, we omit zero entries for large matrices with more complicated block structures. We sometimes write  $0$  and omit entries whenever it helps depict a given matrix block structure.  $I_n$  denotes the identity matrix of order  $n$ . When it is clear from the context, we omit the index and write  $I$ . The vector consisting of all ones, e.g.,  $(1, \dots, 1)^T \in \mathbb{R}^n$ , will be denoted by  $e$ . For a vector  $x \in \mathbb{R}^n$ ,  $X = \text{diag}(x) \in \mathbb{R}^{n \times n}$  denotes the diagonal matrix with  $x$  on its diagonal. For a given matrix  $A \in \mathbb{R}^{m \times n}$  and two subsets  $I \subset \{1, \dots, m\}$ ,  $J \subset \{1, \dots, n\}$ , we refer to the sub-matrix build from  $A$  by taking only the rows/columns indicated by  $I/J$  as  $A_{I, \cdot}$  /  $A_{\cdot, J}$  respectively.

<sup>1</sup>BEAM-ME project: [http://www.beam-me-projekt.de/beam-me/EN/Home/home\\_node.html](http://www.beam-me-projekt.de/beam-me/EN/Home/home_node.html)

<sup>2</sup>UNSEEN project: <https://unseen-project.gitlab.io/home/>

<sup>3</sup>German aerospace center: <https://www.dlr.de/de>

## 2.2 LP, duality and optimality conditions

Consider the following LP in standard form

$$\begin{aligned} \min_x \quad & c^T x \\ \text{subject to} \quad & Ax = b \\ & x \geq 0, \end{aligned}$$

where  $c \in \mathbb{R}^n, b \in \mathbb{R}^m, A \in \mathbb{R}^{m \times n}$ , as well as its associated dual formulation

$$\begin{aligned} \max_{y,z} \quad & b^T y \\ \text{subject to} \quad & A^T y + z = c \\ & z \geq 0, \end{aligned}$$

where  $y \in \mathbb{R}^m, z \in \mathbb{R}^n$ . We assume that all matrices considered here have full rank. It is well-known that if both problems are feasible, the optimal primal and dual objectives coincide [46]. The necessary KKT conditions to either the primal or the dual problem (with motivates the term primal-dual) are given by:

$$A^T y + z - c = 0 \tag{1}$$

$$Ax - b = 0 \tag{2}$$

$$ZXe = 0 \tag{3}$$

$$x, z \geq 0, \tag{4}$$

where  $X = \text{diag}(x)$  and  $Z = \text{diag}(z)$ . All but the complementarity equation eq. (3) are linear.

## 2.3 Introduction to Primal-Dual Interior-Point Methods

In primal-dual infeasible IPMs, perturbed KKT conditions are solved by Newton's method, namely eq. (3) is perturbed by  $\tau > 0$ :

$$ZXe = \tau e. \tag{5}$$

The so-called centrality factor  $\tau$  is successively decreased, which guides the IPM along the so-called *central path* defined by the values of  $\tau$  (close) to the optimal solution until sufficient convergence has been reached. In doing so, the IPM maintains its iterates  $x, z$  strictly within the positive orthant (a fact used later in the computations).

We introduce the vector notation for eqs. (1), (2), (4) and (5) as well as an iteration index  $k$ . At each step of the  $k$  of the IPM, we approximately solve

$$\begin{bmatrix} A^T y^k + z^k \\ Ax^k \\ X^k Z^k e \end{bmatrix} = \begin{bmatrix} c \\ b \\ \tau^k e \end{bmatrix}. \tag{6}$$

The linear system that arises in each iteration  $l$  of Newton's method is

$$\begin{bmatrix} 0 & A^T & I \\ A & 0 & 0 \\ Z^{k,l} & 0 & X^{k,l} \end{bmatrix} \begin{bmatrix} \Delta x^{k,l} \\ \Delta y^{k,l} \\ \Delta z^{k,l} \end{bmatrix} = \begin{bmatrix} r_{x^{k,l}} \\ r_{y^{k,l}} \\ r_{z^{k,l}} \end{bmatrix}, \tag{7}$$

where  $r_{x^{k,l}}, r_{y^{k,l}}, r_{z^{k,l}}$  are residuals right-hand sides. Recalling that  $x^{k,l} > 0$ , we eliminate the last row block

$$\Delta z^{k,l} = (X^{k,l})^{-1} r_{z^{k,l}} - (X^{k,l})^{-1} Z^{k,l} \Delta x^{k,l}, \quad (8)$$

which produces the symmetric so-called *augmented system* [36, 45]

$$\begin{bmatrix} -(X^{k,l})^{-1} Z^{k,l} & A^T \\ A & 0 \end{bmatrix} \begin{bmatrix} \Delta x^{k,l} \\ \Delta y^{k,l} \end{bmatrix} = \begin{bmatrix} \hat{r}_{x^{k,l}} \\ r_{y^{k,l}} \end{bmatrix}. \quad (9)$$

In IPMs for LP, the number of inner iterations for approximately solving eq. (6) is generally kept to a single inner iteration  $l$ , after which the centrality factor  $\tau$  is updated.

## 2.4 The Schur Complement algorithm

Here, we recall the Schur complement algorithm, which was slightly modified for our purpose. We will then use it to derive HSCA. It can be thought of as a block Gaussian elimination. Consider the linear system

$$\begin{bmatrix} K & L \\ L^T & K_0 \end{bmatrix} \begin{bmatrix} x_1 \\ x_0 \end{bmatrix} = \begin{bmatrix} b_1 \\ b_0 \end{bmatrix} \quad (10)$$

with matrices  $K \in \mathbb{R}^{m \times m}$ ,  $L \in \mathbb{R}^{m \times n}$ ,  $K_0 \in \mathbb{R}^{n \times n}$ ,  $n, m \in \mathbb{N}$  and vectors  $x_1, x_0, b_1, b_0$  of appropriate dimensions. We now assume that an implicit factorization of  $K$ , not necessary in the form of actual factors, is available (in fact, we only want to be able to solve  $Kx_1 = b_1$ ). We can compute and factorize the Schur complement of eq. (10) column-wise, as described in algorithm 1, and solve the linear system accordingly.

---

### Algorithm 1 Schur Complement Factorization

---

**Input:** System eq. (10)

- 1: Set  $S = K_0$
  - 2: **for**  $i \in \{1, \dots, n\}$  **do**
  - 3:   Solve  $Kz = L_{:,i}$
  - 4:   Set  $S_{:,i} = S_{:,i} + L^T z$
  - 5: **end for**
  - 6: Factorize  $S$
  - 7: **return**
- 

## 3 A specialized parallel Interior-Point Method

In the remainder of this section, we will show how PIPS-IPM++ employs a parallel Schur complement decomposition [42] to solve eq. (9) in a distributed fashion and in parallel. This forms the basis for the methods presented in section 4.

### 3.1 Message Passing Interface

In the following, we will be relying on the availability of communication between independent processes on a distributed computing system. Our implementation heavily uses the de facto standard in messaging protocols for distributed-memory computing, the message passing interface MPI [13]. MPI provides a set of collective and point-to-point communication routines for a given set of parallel processes. We commonly refer to these processes connected via MPI as *MPI processes* or just *processes*. Each of the MPI processes is assigned a unique global rank in  $0, \dots, N - 1$ , referred to as *global rank*, where  $N$  is the total number of processors. The choice of  $N$  as both the number of blocks and the number of MPI processes is intended, as they are essentially the same (as explained in the following chapters). The global ranks are associated with a global MPI communicator. Generally, communicators are used by processes for collective communication operations such as *Reduce* and *Allreduce*, where a specific reduction operation, e.g., summation, is used to combine the data of all MPI processes on respectively one or all processes. MPI offers the option of creating custom sub-communicators, each of which can contain an arbitrary subset of the  $N$  processes and assigns an additional (communicator-unique) rank to its processes. When discussing a process's rank, we mean its associated global rank (exceptions will be stated explicitly). Throughout this work, we use the Allreduce and Reduce operations to operate on vectors and matrices. Additionally, we use the concept of sub-communicators for the distribution of the linear algebra in HSCA.

### 3.2 A parallel Schur Complement Decomposition

The AHLPs whose system matrix is depicted in fig. 1 can mathematically be described as

$$\begin{aligned}
& \min && c_0^T x_0 + c_1^T x_1 + \dots + c_N^T x_N \\
\text{subject to} && A_0 x_0 &= b_0 \\
&& d_0 \leq C_0 x_0 &\leq f_0 \\
&& A_1 x_0 + B_1 x_1 &= b_1 \\
&& d_1 \leq C_1 x_0 + D_1 x_1 &\leq f_1 \\
&& \vdots & \ddots \quad \quad \quad \vdots \\
&& A_N x_0 + & \quad \quad \quad + B_N x_N = b_N \\
&& d_N \leq C_N x_0 + & \quad \quad \quad + D_N x_N \leq f_N \\
&& F_0 x_0 + F_1 x_1 + \dots + F_N x_N &= b_{N+1} \\
&& d_{N+1} \leq G_0 x_0 + G_1 x_1 + \dots + G_N x_N &\leq f_{N+1} \\
&& & \ell_i \leq x_i \leq u_i \quad \forall i = 0, \dots, N.
\end{aligned} \tag{11}$$

Here  $x_i \in \mathbb{R}^{n_i}$  denote the decision variables,  $c_i \in \mathbb{R}^{n_i}$  the objective vector and  $\ell_i, u_i \in \mathbb{R}^{n_i}$  the variable bounds. The vectors  $b_i \in \mathbb{R}^{m_{iA}}$ ,  $d_i$ , and  $f_i \in \mathbb{R}^{m_{iC}}$  denote the right-hand sides for equalities and lower and upper bounds for inequalities respectively. The system matrix is split into the sub-matrices  $A_i \in \mathbb{R}^{m_{iA} \times n_0}$ ,  $B_i \in \mathbb{R}^{m_{iA} \times n_i}$ ,  $C_i \in \mathbb{R}^{m_{iC} \times n_0}$ ,  $D_i \in \mathbb{R}^{m_{iC} \times n_0}$ ,  $F_i \in \mathbb{R}^{m_{N+1A} \times n_i}$ ,

$G_i \in \mathbb{R}^{m_{N+1C} \times n_i}$  for  $N \in \mathbb{N}$ . We denote by  $n_i \in \mathbb{N}$ , the size of the  $i$ -th primal vector, by  $m_{iA}$  the row dimension of the  $i$ -th equality constraint sub-matrix  $A_i$  and by  $m_{iC} \in \mathbb{N}_0$  the row dimension of the  $i$ -th inequality constraint sub-matrix  $C_i$ .

Using this notation, linking constraints are constraints associated with the blocks  $F_i$  and  $G_i$ , while linking variables are the variables in  $x_0$ . In the following, we will further distinguish linking constraints into *local linking constraints* and *global linking constraints*. Local linking constraints (also called 2-links) only contain non-zeros in  $F_0$  and two consecutive blocks  $F_i$  and  $F_{i+1}$  for exactly one  $i \in \{1, \dots, N-1\}$ . Global linking constraints constitute the rest of the linking constraints, in particular the rows that have entries in  $F_0, F_i, F_j$  where  $|i-j| > 1$  and  $i, j \in \{1, \dots, N\}$ .

For clarity, we will omit the outer and inner iteration indices  $k, l$  introduced for IPMs in the rest of this section. Similarly, we will omit the  $C, D$ , and  $G$  matrices associated with inequality constraints from system eq. (11). Consequently, we refer to the sizes of the remaining  $A_i$  as  $\mathbb{R}^{m_i \times n_0}$ ,  $B_i$  as  $\mathbb{R}^{m_i \times n_i}$  and  $F_i$  as  $\mathbb{R}^{m_{N+1} \times n_i}$ , dropping the matrix index in  $m_{iA}$ .

The augmented system eq. (9) corresponding to eq. (11) is

$$\begin{bmatrix} \Sigma_0 & & & A_0^T & A_1^T & \dots & A_N^T & F_0^T \\ & \Sigma_1 & & & B_1^T & & & F_1^T \\ & & \ddots & & & \ddots & & \vdots \\ & & & \Sigma_N & & & B_N^T & F_N^T \\ A_0 & & & & & & & \\ A_1 & B_1 & & & & & & \\ \vdots & & \ddots & & & & & \\ A_N & & & B_N & & & & \\ F_0 & F_1 & \dots & F_N & & & & \end{bmatrix} \begin{bmatrix} \Delta x_0 \\ \Delta x_1 \\ \vdots \\ \Delta x_N \\ \Delta y_0 \\ \Delta y_1 \\ \vdots \\ \Delta y_N \\ \Delta y_{N+1} \end{bmatrix} = \begin{bmatrix} r_{x_0} \\ r_{x_1} \\ \vdots \\ r_{x_N} \\ r_{y_0} \\ r_{y_1} \\ \vdots \\ r_{y_N} \\ r_{y_{N+1}} \end{bmatrix}, \quad (12)$$

where  $\Sigma_i := -X_i^{-1}Z_i$  for  $i = 0, \dots, N$ , a common notation in the IPM literature. After symmetric permutation, the system becomes:

$$\begin{bmatrix} K_1 & & L_1 \\ & \ddots & \vdots \\ & & K_N & L_N \\ L_1^T & \dots & L_N^T & K_0 \end{bmatrix} \begin{bmatrix} \Delta z_1 \\ \vdots \\ \Delta z_N \\ \Delta z_0 \end{bmatrix} = \begin{bmatrix} b_1 \\ \vdots \\ b_N \\ b_0 \end{bmatrix} \quad (13)$$

where

$$K_i = \begin{bmatrix} \Sigma_i & B_i^T \\ B_i & 0 \end{bmatrix}, \quad K_0 = \begin{bmatrix} \Sigma_0 & A_0^T & F_0^T \\ A_0 & 0 & 0 \\ F_0 & 0 & 0 \end{bmatrix}, \quad L_i = \begin{bmatrix} 0 & 0 & F_i^T \\ A_i & 0 & 0 \end{bmatrix}, \quad (14)$$

and

$$\Delta z_0 = \begin{bmatrix} \Delta x_0 \\ \Delta y_0 \\ \Delta y_{N+1} \end{bmatrix}, \quad \Delta z_i = \begin{bmatrix} \Delta x_i \\ \Delta y_i \end{bmatrix}, \quad b_0 = \begin{bmatrix} r_{x_0} \\ r_{y_0} \\ r_{y_{N+1}} \end{bmatrix}, \quad b_i = \begin{bmatrix} r_{x_i} \\ r_{y_i} \end{bmatrix} \quad (15)$$

for  $i = \{1, \dots, N\}$ . As described in [42], this system can be solved efficiently in parallel using a Schur complement decomposition.

As usual in direct methods, we distinguish between two phases, *factor* and *solve*. The factorization phase for solving system 13 is described by algorithm 2. The solve phase for a given right-hand side is described by algorithm 3.

---

**Algorithm 2** *Parallel factorization*

---

**Input:** System matrix eq. (13)

- 1: *Factorize*  $K_i$  for all  $i \in \{1, \dots, N\}$
  - 2: *Compute*  $-L_i^T K_i^{-1} L_i$  for all  $i \in \{1, \dots, N\}$
  - 3: Sum Schur complement  $S := K_0 - \sum_{i=1}^N L_i^T K_i^{-1} L_i$
  - 4: Factorize  $S$
  - 5: **return**
- 

---

**Algorithm 3** *Parallel solve*

---

**Input:** Factorized system from algorithm 2 and right hand side in eq. (13)

**Output:** Solution  $\Delta z_i$ ,  $i \in \{0, \dots, N\}$

- 1: *Compute*  $-L_i^T K_i b_i$  for all  $i \in \{1, \dots, N\}$
  - 2: Sum Schur complement right hand side  $\hat{b}_0 = b_0 - \sum_{i=1}^N L_i^T K_i b_i$
  - 3: Solve  $S \Delta z_0 = \hat{b}_0$
  - 4: *Compute modified right-hand sides*  $\hat{b}_i = b_i - L_i \Delta z_0$
  - 5: *Solve*  $K_i \Delta z_i = \hat{b}_i$  for all  $i \in \{1, \dots, N\}$
  - 6: **return**
- 

Algorithm 2 extends algorithm 1 in PIPS-IPM++. In its first implementation, PIPS-IPM++ used a combination of algorithm 1 and algorithm 2 to compute the Schur complement. Currently, the faster way of computing the blockwise Schur complement contributions is an incomplete LU factorization routine [40] implemented in the solver PARDISO [1, 7, 6].

lines 1 and 2 of algorithm 2, and lines 1, 4 and 5 from algorithm 3 can be executed in parallel and are highlighted in italic. When each MPI process has access to the data needed for the parallel steps, all steps but the Schur complement factorization, and the Schur complement solve can be run in distributed parallel. In addition, not every process needs a representation of the problem: process  $i$  requires knowledge of the blocks  $i$  and 0. This induces a natural limit on the number of processes being used and motivates the slightly ambiguous notation of  $N$  as both the number of processes and the number of blocks in the problem. The problem can be distributed within this decomposition among at most  $N$  processes. We point out that line 3 in algorithm 2 and line 2 in algorithm 3 require communication among the processes to form the Schur complement and its right-hand side. Traditionally, the Schur complement in PIPS-IPM++ has been stored on a single dedicated process, which makes the communication in both steps a *reduce operation* (as compared to an *allreduce operation*). This was mainly done to save memory and computing power on individual nodes since running PIPS-IPM++ with one process per node is highly inefficient and expensive regarding resources. We point out that processing the Schur complement on a single MPI process requires additional communication (*scatter*) of the solution  $z_0$  in line 3 of algorithm 3. We will always assume that  $N$  MPI processes are used for simplicity, so the number of blocks and processes coincide.



The Schur complement (line 3 in algorithm 2) now has the following structure:

$$\begin{aligned}
L_i^T K_i^{-1} L_i &= \begin{bmatrix} 0 & A_i^T \\ 0 & 0 \\ \hat{F}_i & 0 \\ \mathbf{F}_i & 0 \end{bmatrix} \begin{bmatrix} \tilde{K}_{1,1}^i & \tilde{K}_{1,2}^i \\ \tilde{K}_{2,1}^i & \tilde{K}_{2,2}^i \end{bmatrix} \begin{bmatrix} 0 & 0 & \hat{F}_i^T & \mathbf{F}_i^T \\ A_i & 0 & 0 & 0 \end{bmatrix} \\
&= \begin{bmatrix} A_i^T \tilde{K}_{2,2}^i A_i & 0 & A_i^T \tilde{K}_{2,1}^i \hat{F}_i^T & A_i^T \tilde{K}_{2,1}^i \mathbf{F}_i^T \\ 0 & 0 & 0 & 0 \\ F_i \tilde{K}_{1,2}^i A_i & 0 & \hat{F}_i \tilde{K}_{1,1}^i \hat{F}_i^T & \hat{F}_i \tilde{K}_{1,1}^i \mathbf{F}_i^T \\ \mathbf{F}_i \tilde{K}_{1,2}^i A_i & 0 & \mathbf{F}_i \tilde{K}_{1,1}^i \hat{F}_i^T & \mathbf{F}_i \tilde{K}_{1,1}^i \mathbf{F}_i^T \end{bmatrix} \\
F_i \tilde{K}_{1,1}^i F_i^T &= \begin{bmatrix} \vdots \\ 0 \\ \mathcal{F}'_{i-1} \\ \mathcal{F}_i \\ 0 \\ \vdots \end{bmatrix} \tilde{K}_{1,1}^i [\dots 0 \mathcal{F}'_{i-1}{}^T \mathcal{F}_i^T 0 \dots] = \\
&\begin{bmatrix} \ddots & \vdots & \vdots & \vdots & \ddots \\ \dots & 0 & 0 & 0 & \dots \\ \dots & \mathcal{F}'_{i-1} \tilde{K}_{1,1}^i \mathcal{F}'_{i-1}{}^T & \mathcal{F}'_{i-1} \tilde{K}_{1,1}^i \mathcal{F}_i^T & 0 & \dots \\ \dots & \mathcal{F}_i \tilde{K}_{1,1}^i \mathcal{F}'_{i-1}{}^T & \mathcal{F}_i \tilde{K}_{1,1}^i \mathcal{F}_i^T & 0 & \dots \\ \dots & 0 & 0 & 0 & \dots \\ \ddots & \vdots & \vdots & \vdots & \ddots \end{bmatrix}.
\end{aligned}$$

Summing up these individual Schur complement contributions (and after appropriate symmetric permutation), the final Schur complement is expressed as the following block matrix:

$$P^T \left( \sum_{i=1}^N L_i^T K_i^{-1} L_i \right) P = \begin{bmatrix} M_1 & H_1^T & & & & E_1^T & 0 \\ H_1 & M_2 & H_2^T & & & E_2^T & 0 \\ & H_2 & \ddots & \ddots & & \vdots & \vdots \\ & & \ddots & & H_{N-2}^T & E_{N-2}^T & 0 \\ & & & H_{N-2} & M_{N-1} & E_{N-1}^T & 0 \\ E_1 & E_2 & \dots & E_{N-1} & E_{N-1} & M_0 & 0 \\ 0 & 0 & \dots & 0 & 0 & 0 & 0 \end{bmatrix}. \quad (19)$$

The submatrices in eq. (19) are defined as

$$\begin{aligned}
M_i &= \mathcal{F}_i \tilde{K}_{1,1}^i \mathcal{F}_i^T + \mathcal{F}'_i \tilde{K}_{1,1}^{i+1} \mathcal{F}'_i{}^T, \\
E_i &= \begin{bmatrix} \mathbf{F}_i \tilde{K}_{1,1}^i \mathcal{F}_i^T + \mathbf{F}_{i+1} \tilde{K}_{1,1}^{i+1} \mathcal{F}_i^T \\ A_i^T \tilde{K}_{2,1}^i \mathcal{F}_i^T + A_{i+1}^T \tilde{K}_{2,1}^{i+1} \mathcal{F}_i^T \end{bmatrix}, \quad (20)
\end{aligned}$$

for  $i \in \{1, \dots, N-1\}$  and

$$H_i = \mathcal{F}_{i+1} \tilde{K}_{1,1}^{i+1} \mathcal{F}_i^T,$$



We can apply a Schur complement decomposition to this system by setting

$$K_0 = \begin{bmatrix} \Sigma_0 & A_0^T & \mathbf{F}_0^T \\ A_0 & 0 & 0 \\ \mathbf{F}_0 & 0 & 0 \end{bmatrix}$$

in eq. (10). We call the Schur complement system obtained this way the dense layer of our multi-layered Schur complement decomposition. Given an implicit factorization of the resulting inner system in eq. (10), we can use algorithm 1 to obtain an implicit factorization of the whole system. In this case, the Schur complement has the same structure as eq. (19) but without the parts associated with two-links. Thus, as long as no additional structure is known, only the  $A_0$  part of the resulting Schur complement can be deemed sparse. In our implementation, the Schur complement of the dense layer of the hierarchical decomposition is treated as a dense matrix and factorized by the dedicated LAPACK routine. An upper bound on its number of non-zeros is given by the square of its dimension  $(m_{\mathbf{F}} + n_0 + m_0)^2$ . Using a Schur complement to mitigate the fill-in generated by dense columns in IPMs is usually applied when solving the *normal equations* [4, 38]. When solving the *augmented system*, dense columns are usually treated by adapting the choice of pivoting. The method presented here can be seen as a similar approach [36].

## 4.2 The Inner Linear Systems

To actually apply algorithm 1 to the dense layer, as presented in the previous chapter, we must be able to solve equations with the inner linear system

$$\left[ \begin{array}{cc|c} \Sigma_1 & B_1^T & \hat{F}_1^T \\ B_1 & 0 & 0 \\ & \ddots & \\ & & \Sigma_N & B_N^T & \hat{F}_N^T \\ & & B_N & 0 & 0 \\ \hline \hat{F}_1 & 0 & \hat{F}_N & 0 & 0 \end{array} \right] \begin{bmatrix} \Delta x_1 \\ \Delta y_1 \\ \vdots \\ \Delta x_N \\ \Delta y_N \\ \Delta y_0 \end{bmatrix} = \begin{bmatrix} r_{x_1} \\ r_{y_1} \\ \vdots \\ r_{x_N} \\ r_{y_N} \\ r_{y_0} \end{bmatrix}. \quad (23)$$

Since eq. (23) has the same structure as eq. (13), we could solve it using the parallel factorization and solve (algorithms 2 and 3). These two layered linear systems are the simplest case of the hierarchical solution approach.

To distribute and parallelize the solution process further, we split the linear system and apply recursive Schur complement decomposition by permuting subsets of the two-link constraints “into” eq. (23). We recall the structure of

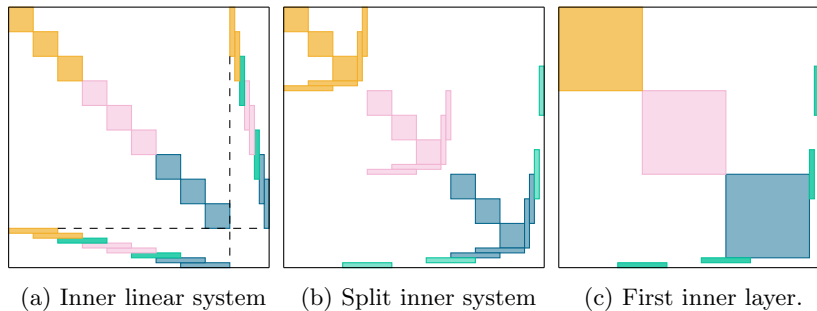


Figure 2: Permuting the inner linear system.

eq. (23) with expanded linking constraints:

$$\left[ \begin{array}{ccc|ccc}
 \Sigma_1 & B_1^T & & \mathcal{F}_1^T & 0 & \\
 B_1 & 0 & & 0 & 0 & \\
 & & \Sigma_2 & B_2^T & & \\
 & & B_2 & 0 & & \\
 & & & \ddots & & \ddots \\
 & & & & \Sigma_N & B_N^T & & \mathcal{F}_{N-1}^{T'} & \\
 & & & & B_N & 0 & & 0 & \\
 \hline
 \mathcal{F}_1 & 0 & \mathcal{F}'_1 & 0 & & & & & \\
 0 & 0 & \mathcal{F}_2 & 0 & & & & 0 & \\
 & & & \ddots & & & & & \\
 & & & & \mathcal{F}'_{N-1} & 0 & & & 
 \end{array} \right] \begin{bmatrix} \Delta x_1 \\ \Delta y_1 \\ \vdots \\ \Delta x_N \\ \Delta y_N \\ \Delta y_{0,1} \\ \vdots \\ \Delta y_{0,N-1} \end{bmatrix} = \begin{bmatrix} r_{x_1} \\ r_{y_1} \\ \vdots \\ r_{x_N} \\ r_{y_N} \\ r_{y_{0,1}} \\ \vdots \\ r_{y_{0,N-1}} \end{bmatrix}. \quad (24)$$

This system is schematically shown in fig. 2a. Here, we are given a system with nine diagonal blocks. We divide this system into three smaller ones. For this purpose, we colored the components belonging to each subsystem with the same color. By permuting all local linking constraints but the ones linking the subsystems (depicted in green) further into the system, we obtain the system in fig. 2b. Interpreting the system in fig. 2b as displayed in fig. 2c, we can use algorithm 1 for its factorization. We call this system the top-most inner system. As the diagonal blocks of this system themselves exhibit the same structure as the original PIPS-IPM++ system eq. (13), we can use (algorithms 2 and 3) for factorization and solution. We call the systems arising from the block-diagonal factorization the leaf systems.

While the structure of the leaf systems allows for the application of the original PIPS-IPM++ algorithms, it also provides for the application of the same permutation and split as in fig. 2. This would create another layer in the Schur complement decomposition and further shrink the leaf systems. Given enough blocks, this enables an arbitrary amount of layers. In practice, the recursive Schur complement decomposition affects the computational cost of a linear system solve and must be weighed against the benefit of smaller Schur complements and their distributed computation. We have not encountered systems or problems where more than four layers were beneficial. In the remainder of this section, we explain the permutation and split of the system with more mathematical rigorosity.

Partitioning the blocks of eq. (24) into  $\{1, \dots, N\}$  into  $i_0 = -1 < i_1 < i_2 < \dots < i_{k+1} = N$ ,  $k \in \mathbb{N}$  we obtain the following system matrix (see fig. 2b)

$$\left[ \begin{array}{ccc|ccc} K_1 & & & & 0 & \\ & & & & \mathcal{F}_{i_1}^T & \\ & & & & 0 & \\ & K_2 & & & \mathcal{F}_{i_1}^{T'} & 0 \\ & & & & 0 & \mathcal{F}_{i_2}^T \\ & & & & 0 & 0 \\ & & \ddots & & & \ddots \\ & & & & & \mathcal{F}_{i_{k-1}}^{T'} \\ & & & K_k & & 0 \\ \hline \tilde{B}_1^T & \tilde{B}_2^T & \dots & \tilde{B}_k^T & & 0 \\ \hline 0 & \mathcal{F}_{i_1} & 0 & \mathcal{F}'_{i_1} & 0 & 0 \\ & & 0 & \mathcal{F}_{i_2} & 0 & \\ & & & \ddots & & \\ & & & & \mathcal{F}'_{i_{k-1}} & 0 & 0 \end{array} \right] := \left[ \begin{array}{ccc|ccc} K_1 & & & & 0 & \\ & K_2 & & & \mathcal{F}_{i_1}^{T'} & 0 \\ & & & & 0 & \mathcal{F}_{i_2}^T \\ & & \ddots & & & \ddots \\ & & & K_k & & \mathcal{F}_{i_{k-1}}^{T'} \\ \hline \tilde{B}_1^T & \tilde{B}_2^T & \dots & \tilde{B}_k^T & & 0 \\ \hline 0 & \mathcal{F}_{i_1} & 0 & \mathcal{F}'_{i_1} & 0 & 0 \\ & & 0 & \mathcal{F}_{i_2} & 0 & \\ & & & \ddots & & \\ & & & & \mathcal{F}'_{i_{k-1}} & 0 & 0 \end{array} \right], \quad (25)$$

where the diagonal blocks themselves exhibit a block-diagonal system structure and are defined as:

$$K_j := \left[ \begin{array}{ccc|ccc} \Sigma_{i_{j-1}+1} & B_{i_{j-1}+1}^T & & & \mathcal{F}_{i_{j-1}+1}^T & 0 \\ B_{i_{j-1}+1} & 0 & & & 0 & 0 \\ & & \Sigma_{i_{j-1}+2} & B_{i_{j-1}+2}^T & \mathcal{F}_{i_{j-1}+1}^{T'} & \mathcal{F}_{i_{j-1}+2}^T \\ & & B_{i_{j-1}+2} & 0 & 0 & 0 \\ & & & \ddots & & \ddots \\ & & & & \Sigma_{i_j} & B_{i_j}^T \\ & & & & B_{i_j} & 0 \\ \hline \mathcal{F}_{i_{j-1}+1} & 0 & \mathcal{F}'_{i_{j-1}+1} & 0 & & \mathcal{F}_{i_{j-1}}^{T'} \\ 0 & 0 & \mathcal{F}_{i_{j-1}+2} & 0 & & 0 \\ & & & \ddots & & \\ & & & & \mathcal{F}'_{i_{j-1}} & 0 \end{array} \right]. \quad (26)$$

As described earlier, we have decomposed the inner linear system into  $k$  smaller linear systems with the system matrices  $K_i$ . These block-diagonal leaf systems are decoupled in the sense that for every block  $j \in \{1, \dots, k\}$ , the processes  $i_{j-1}, \dots, i_j$  can factorize and solve the leaf system  $K_j$  independently of the other processes. The factorization of the lower-level systems only requires communication between the processes related to the respective blocks of the system and can, therefore, be done in parallel among the process groups.

The Schur complements corresponding to this split all have the same structure as in eq. (19). As none of the inner linear systems eq. (26) or eq. (25) contain any global linking constraints, e.g., the  $E_i$  blocks in eq. (19) are not present, their Schur complements are mostly sparse. For example, the Schur



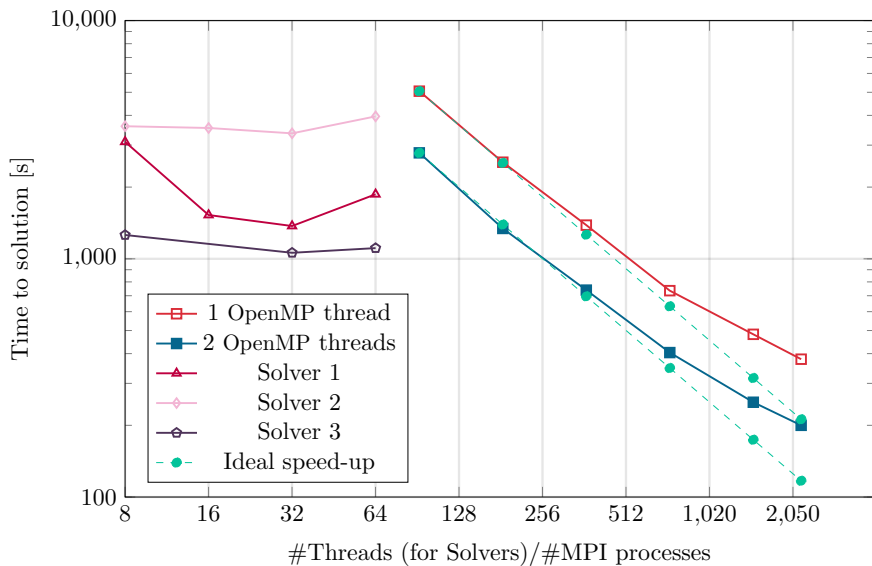


Figure 3: Scaling behavior of all solvers on MISO\_DISP\_488.

the latest incomplete LU factorization approach applied in [40, 42] and originally used within PIPS-IPM++. Generally, we observed that the factorization routine of MA57 was much slower than the one in PARDISO, especially as the linear systems grow in size. Additionally, we lose PARDISO’s significant speed-up when computing the bottommost Schur complement contributions with the parallelized incomplete Schur complement computation. PARDISO is also more robust when solving rank-deficient linear systems. While MA57 itself is purely sequential, we leverage its thread-safeness and OpenMP to solve multiple right-hand sides in parallel by calling MA57 from different threads with the same factorization. Factorization is obtained beforehand using a single thread. In our experience, this type of parallelization scales much better (and is faster) than the parallel factorization routines of all the other solvers we tried.

### The scaling behavior of the hierarchical approach

We first assess the scaling behavior of our implementation. In fig. 3 we show the behavior of our solver on the *MISO\_DISP\_488* instance as well as the scaling behavior of the three commercial but academically available solvers CPLEX 22.1.1.0 [30], Gurobi11 [28], and the Cardinal Optimizer COPT 7.2.3 [19]. We solved the instance with PIPS-IPM++ multiple times using a different number of MPI processes and OpenMP threads and (implicitly) cluster nodes. The problem displayed has 120 million nonzeros, 25 million columns, and 12 million rows and is split into 2,190 blocks, which limits the number of usable MPI processes to 2,190. Notably, the instance contains roughly 55,000 linking constraints, and the initial symbolic analysis of the Schur complement in PIPS-IPM++ determined an upper bound of 100,424,258 nonzeros. This made the instance intractable for the original PIPS-IPM++ algorithm (see table 1). We adapted the number of threads for each solution for the commercial solvers while turning off crossover

and using barrier as the optimization algorithm. Both PIPS-IPM++ and the commercial solvers were set to solve the LP up to a convergence tolerance of  $10^{-6}$ .

Additionally, we plot the optimal speed-up for each scenario as a dotted line. Our approach is not expected to achieve linear speed-up, as the mid-level Schur complements are solved by only a subset of threads in parallel, and the root-level Schur complement is solved sequentially. However, the hierarchical solution approach achieves a strong near-linear speed-up on the given instance. Additionally, PIPS-IPM++ benefits from adding a second OpenMP thread while solving. More OpenMP threads did not produce much speed-up over the 2-thread variant for the given instance. It can also be observed, that the commercial solvers do not scale well with the availability of more compute resources. Each solver runs fastest with 32 threads, which we attribute to the memory-boundedness of the Cholesky factorization underlying the IPM.

### Impact of block sizes on the performance of hierarchical approach vs. original approach

The performance of both the original PIPS-IPM++ and the hierarchical approach are heavily problem-dependent. Given the superior performance of PARDISO on large linear systems, PIPS-IPM++ is largely favored on systems with a manageable number of linking constraints and large blocks of constraints. On the other hand, the hierarchical extension struggles with large Schur complements and large diagonal blocks since MA57 is the slower linear solver. Also, fewer blocks mean less potential for distributing and shrinking the Schur complement, the main idea of the hierarchical approach. In a way, both approaches complement one another, being efficient on mutually exclusive problem classes. Depending on how the modeler splits a given model into blocks, one approach may outperform the other even in the same instance. This depends on multiple factors: the available compute resources, the amount of dense linking constraints, and the availability of a fast linear solver (suited for either approach).

We conducted a simple experiment on four medium *SIMPLE* instances with different sizes (fig. 4). From the top left to the bottom right, the instances become increasingly more difficult to solve due to the growing size of the diagonal blocks. The number of linking constraints in the problem, when split into a certain number of blocks, remained constant over all instances. Each instance can theoretically be split into 8,760 blocks. Combining multiple blocks into one decreases the number of linking constraints in the Schur complement approach. We solved each instance with the original PIPS-IPM++ and our new approach, split into five different amounts of blocks: 365, 730, 1,460, 2,920, and 8,760. In this setting, fewer blocks automatically means bigger diagonal blocks and, as pointed out before, smaller global Schur complements. For each of the four instances, the original approach benefits from large diagonal blocks but experiences a significant slowdown with a growing number of linking constraints. On the other hand, the performance of the hierarchical approach is more insensitive to the increasing number of linking constraints when splitting the instances more finely. This is expected as the amount of parallel work decreases but at a much lower rate than for the original implementation. In the hierarchical approach (in an ideal setting), the number of local linking constraints in each of the Schur complements only grows in  $\mathcal{O}(\sqrt{n})$  (with  $n$  denoting the number

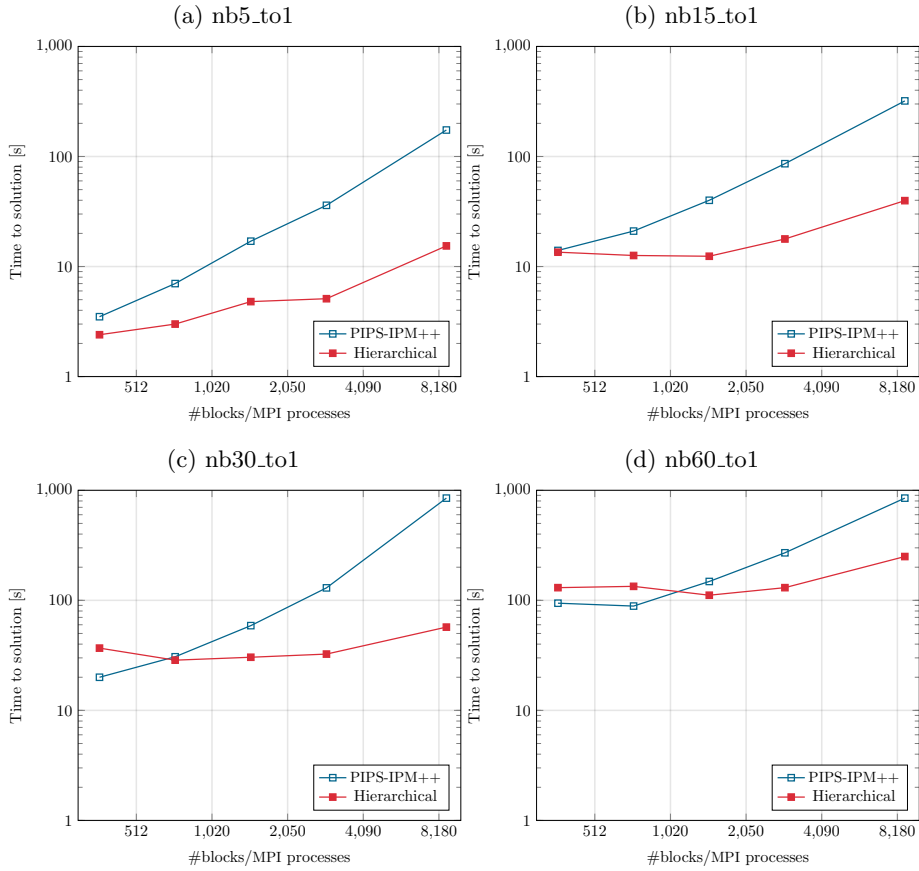


Figure 4: Comparison of the original PIPS-IPM++ and the hierarchical approach for different block sizes and constant amount of linking constraints.

of local linking constraints), as compared to  $\mathcal{O}(n)$  for the original approach.

At the same time, the hierarchical approach is worse at handling larger diagonal blocks and large Schur complements. While it can outperform the original PIPS-IPM++ for the smaller two instances, its superiority becomes more apparent as the diagonal block sizes are larger. For the hardest (in terms of diagonal block size) two instances, the original PIPS-IPM++ cannot be beaten by the hierarchical approach. In the other two instances, where the ratio of diagonal block size to the number of linking constraints favors the hierarchical approach, the original algorithm consistently outperforms. Once more, the optimal approach strongly depends on the individual layout of the given instance.

There are two scenarios where we expect the hierarchical approach, given sufficient compute resources, to consistently outperform the original PIPS-IPM++. First, should a user not have access to a high-performance (commercial) sparse direct linear solver like PARDISO but to (say) MA57, the hierarchical approach should usually be picked over the original PIPS-IPM++. A more lightweight solver will benefit from smaller matrices and scale well within the hierarchical approach. Second, in distributed but memory-bound environments, such as the

JUWELS supercomputer, large Schur complements can usually not be factorized practically/efficiently, and the only solution method available is the hierarchical extension. In all other circumstances, the out-performance of either approach will be model-dependent.

## Solution times of hierarchical approach on intractable models

Lastly, we present experiments on models that the original implementation of PIPS-IPM++ could not efficiently solve. In table 1, we compare solution times obtained with the hierarchical approach, the original PIPS-IPM++, and the three commercial solvers, CPLEX 22.1.1.0, Gurobi11, and COPT 7.2.3 each run with 32 threads. Apart from the run time, we list model properties for each instance: the number of variables, constraints, nonzeros, and linking constraints (shortened as *link. cons.*). We write MEM whenever PIPS-IPM++ crashes due to memory limitations on the compute nodes. For MISO\_DISP\_120 and MISO\_DISP\_488, we could not obtain results with the original PIPS-IPM++ due to an error in underlying software packages. For these same instances, Solver 2 could not obtain optimal solutions but instead returned sub-optimal ones. The respective times are marked with '\*'. The amount of nodes used to obtain these results varies between 30 and 60. For SIMPLE\_4, the hierarchical approach splits the Schur complement into 4 layers and 3 for the other instances.

Instance	Size				Run time (seconds)				
	variables	constraints	nonzeros	link. cons.	HSCA	PIPS	Solver 1	Solver 2	Solver 3
SIMPLE_1	5 790 840	5 264 881	20 941 510	525 600	561	849	461	704	717
SIMPLE_2	5 785 000	5 259 041	20 935 670	175 200	121	278	479	710	744
SIMPLE_3	59 795 108	51 604 093	205 569 328	71 680	922	400	4 571	8 076	5 368
SIMPLE_4	76 180 100	59 798 125	254 718 160	1 679 371	2 343	MEM	6 555	7 902	6 555
MISO_EXP_30	4 801 730	5 055 872	19 423 706	96 388	76	MEM	795	855	647
MISO_EXP_120	14 563 124	15 351 736	57 902 536	311 040	741	MEM	4 690	12 391	3 235
MISO_EXP_240	22 369 314	26 401 302	98 388 377	1 156 398	1 392	MEM	12 252	25 391	10 624
MISO_DISP_120	11 321 189	12 109 847	45 987 257	48 240	48	-	627	1 037*	397
MISO_DISP_488	25 444 088	11 794 384	120 094 317	54 844	206	MEM	1 373	3 363*	1 060

Table 1: Computational results for large-scale instances.

In line with the results presented in [42], PIPS-IPM++ and the hierarchical approach often outperform commercial software. This is especially visible in real-world MISO instances and larger SIMPLE instances. Overall, the hierarchical approach can achieve speed-ups of up to a factor of 15 in the presented instances. Similar to fig. 4, we see that for the instances SIMPLE\_2 and SIMPLE\_3, either approach can outperform the other. This depends on the amount of linking constraints vs. the size of the diagonal blocks. PIPS-IPM++ cannot efficiently solve many instances as it often runs out of memory when factorizing the Schur complement. None of the instances could be solved using the original PIPS-IPM++ and MA57 instead of PARDISO.

We finally note that the performance of the commercial solvers often also strongly depends on their ability to presolve the instances. They usually can reduce the problem size significantly more than PIPS-IPM++. This has mainly two reasons. First, PIPS-IPM++ presolve is designed not to destroy the underlying problem structure of an instance [22]. This mostly leads to limitations when

aggregating variables in between blocks. Second, PIPS-IPM++ current presolve only implements a handful of methods - far from what is available in modern commercial LP solvers. As a result, the presolved problems in PIPS-IPM++ are often more challenging and exhibit higher redundancy than their commercial counterparts.

## 6 Conclusions

This paper presents HSCA, a novel distributed approach for efficiently solving large arrow-head structured LPs. It is based on the efficient distributed factorization of the KKT system of an IPM. Our approach exploits our models' primal-dual block-angular problem structure to distribute and parallelize the underlying linear algebra. Extending the original PIPS-IPM++ implementation, we applied a multi-level Schur complement decomposition to deal with problems with up to one million linking constraints. We showed the limits of our approach and discussed scenarios in which either implementation outperforms the other. While HSCA often outperforms commercial solvers and the original PIPS-IPM++, its performance is heavily problem-dependent. In this, HSCA behaves complementary to the original PIPS-IPM++ and should be considered an alternative when solving large-scale arrowhead LPs. Good scalability is the key feature that gives PIPS-IPM++ and its hierarchical extension an edge over other commercial optimization software. As demonstrated, most commercial software does not scale well with additional threads and cores. With increasingly more affordable and efficient hardware, scalable numerical algorithms are bound to outperform and replace traditional solution methods, even if they have a higher total computational cost.

While the first implementation of the hierarchical approach has already achieved promising results, several other research paths remain. First, presolve is still very limited and a full presolve suite would improve both run time and stability of our solver and would make it more comparable to commercial software. Second, we are still exploring options for the underlying linear solver with which we might be able to improve PIPS-IPM++ performance. Third, as HSCA is not limited to 2-link constraints, a more elaborate structure detection could be further implemented. In particular, one could account for linking variables and constraints linking  $n$  consecutive blocks, leading to a more complicated Schur complement structure. The IPM algorithm, discussed briefly by this paper, could also be further improved. To this end, we plan on implementing a sequential version of PIPS-IPM++ to robustify the IPM and compare its performance against the performance of other codes. Last, many open questions remain to be addressed on the application side. In the ongoing research project Peregrine<sup>4</sup> we are integrating automatic structure detection, similar to the work done in [8], into our software, as currently the modeler is responsible for annotating the models' block structure. Lastly, we are preparing an open model library containing large-scale ESMs, which will also include the problems used in this paper. We invite others to try out our software and contribute; the version used in this paper is available on GitHub.

---

<sup>4</sup><https://www.dlr.de/en/ve/research-and-transfer/projects/project-peregrine>

## Acknowledgements

The described research activities are funded by the Federal Ministry for Economic Affairs and Energy within the project UNSEEN (ID: 03EI1004C, 03EI1004D). The authors gratefully acknowledge the Gauss Centre for Supercomputing e.V. ([www.gauss-centre.eu](http://www.gauss-centre.eu)) for funding this project by providing computing time through the John von Neumann Institute for Computing (NIC) on the GCS Supercomputer JUWELS at Jülich Supercomputing Centre (JSC). We thank Charlie Vanaret for fruitful discussions and his fierce effort to make this paper more readable.

## References

- [1] Alappat et al. A recursive algebraic coloring technique for hardware-efficient symmetric sparse matrix-vector multiplication. *ACM Trans. Parallel Comput.*, 7(3), June 2020.
- [2] Amestoy et al. A fully asynchronous multifrontal solver using distributed dynamic scheduling. *SIAM J. Matrix Anal. Appl.*, 23(1):15–41, 2001.
- [3] Amestoy et al. Performance and Scalability of the Block Low-Rank Multifrontal Factorization on Multicore Architectures. *ACM Trans. Math. Softw.*, 45:2:1–2:26, 2019.
- [4] Knud D. Andersen. A modified schur-complement method for handling dense columns in interior-point methods for linear programming. *ACM Trans. Math. Softw.*, 22(3):348–356, sep 1996.
- [5] Robert E. Bixby. Solving real-world linear programs: A decade and more of progress. *Oper. Res.*, 50(1):3–15, 2002.
- [6] Bollhöfer et al. Large-scale sparse inverse covariance matrix estimation. *SIAM J. Sci. Comput.*, 41(1):A380–A401, 2019.
- [7] Bollhöfer et al. *State-of-the-Art Sparse Direct Solvers*, pages 3–33. Springer International Publishing, Cham, 2020.
- [8] Ralf Borndörfer, Carlos E. Ferreira, and Alexander Martin. Decomposing matrices into blocks. *SIAM J. Optim.*, 9(1):236–269, 1998.
- [9] K. Cao, J. Metzdorf, and S. Birbalta. Incorporating Power Transmission Bottlenecks into Aggregated Energy System Models. *Sustainability*, 10(6):1–32, 2018.
- [10] Jordi Castro. A specialized interior-point algorithm for multicommodity network flows. *SIAM J. Optim.*, 10(3):852–877, 2000.
- [11] Jordi Castro. Interior-point solver for convex separable block-angular problems. *Optim. Methods Softw.*, 31(1):88–109, 2016.
- [12] V. Chvátal. *Linear Programming*. Series of books in the mathematical sciences. W. H. Freeman, 1983.

- [13] Lyndon Clarke, Ian Glendinning, and Rolf Hempel. The mpi message passing interface standard. In *Programming Environments for Massively Parallel Distributed Systems*, pages 213–218, 1994.
- [14] Marco Colombo and Jacek Gondzio. Further development of multiple centrality correctors for interior point methods. *Comput. Optim. Appl.*, 41(3):277–305, Dec 2008.
- [15] Leonardo Dagum and Ramesh Menon. Openmp: an industry standard api for shared-memory programming. *IEEE Comput. Sci. Eng.*, 5(1):46–55, 1998.
- [16] Iain S. Duff. Ma57—a code for the solution of sparse symmetric definite and indefinite systems. *ACM Trans. Math. Softw.*, 30(2):118–144, jun 2004.
- [17] Iain S. Duff and John Ker Reid. Ma27 – a set of fortran subroutines for solving sparse symmetric sets of linear equations, 1982.
- [18] Lustig et al. On implementing mehrotra’s predictor–corrector interior-point method for linear programming. *SIAM J. Optim.*, 2(3):435–449, 1992.
- [19] Ge et al. Cardinal optimizer user guide, 2023.
- [20] Hans Christian Gils et al. Remix: A gams-based framework for optimizing energy system models. *JOSS preprint*, 2023.
- [21] Gils et al. Integrated modelling of variable renewable energy-based power supply in europe. *Energy*, 123:173–188, 2017.
- [22] Gleixner et al. First experiments with structure-aware presolving for a parallel interior-point method. In *Oper. Res. Proc.*, pages 105–111. Springer, 2020.
- [23] Jacek Gondzio. Interior point methods 25 years later. *EJOR Eur. J. Oper. Res.*, 218(3):587–601, 2012.
- [24] Jacek Gondzio and Andreas Grothey. Parallel interior-point solver for structured quadratic programs: Application to financial planning problems. *Ann. Oper. Res.*, 152:319–339, 07 2007.
- [25] Jacek Gondzio and Andreas Grothey. Exploiting structure in parallel implementation of interior point methods for optimization. *Comput Manag Sci* 6, page 135–160, 2009.
- [26] Michael D. Grigoriadis and Leonid G. Khachiyan. An interior point method for bordered block-diagonal linear programs. *SIAM J. Optim.*, 6(4):913–932, 1996.
- [27] Anshul Gupta. Wsmp: Watson sparse matrix package. part i - direct solution of symmetric sparse systems version 1.0.0, 2000.
- [28] Gurobi Optimization, LLC. Gurobi Optimizer, 2023.
- [29] J. Hogg and Jennifer A. Scott. An indefinite sparse direct solver for large problems on multicore machines. *Rutherford Appleton Laboratory Technical Reports*, 2010.

- [30] IBM ILOG. Cplex 22.1.2, 2024.
- [31] Intel Corporation. Intel math kernel library, 2024.
- [32] Jülich Supercomputing Centre. JUWELS: Modular Tier-0/1 Supercomputer at the Jülich Supercomputing Centre. *Journal of large-scale research facilities*, 5(A135), 2019.
- [33] Kim et al. An asynchronous bundle-trust-region method for dual decomposition of stochastic mixed-integer programming. *SIAM J. Optim.*, 29(1):318–342, 2019.
- [34] M. Lubin, C. G. Petra, Mihai Anitescu, and V. M. Zavala. Scalable stochastic optimization of complex energy systems. In *11 ACM/IEEE Supercomputing Conference*, 2011.
- [35] Lubin et al. On parallelizing dual decomposition in stochastic integer programming. *Oper. Res. Lett.*, 41(3):252–258, 2013.
- [36] István Maros and Csaba Mészáros. The role of the augmented system in interior point methods. *EJOR Eur. J. Oper. Res.*, 107(3):720–736, 1998.
- [37] Sanjay Mehrotra. On the implementation of a primal-dual interior point method. *SIAM J. Optim.*, 2(4):575–601, 1992.
- [38] Csaba Mészáros. Detecting “dense” columns in interior point methods for linear programs. *Comput. Optim. Appl.*, 36(2–3):309–320, apr 2007.
- [39] Jorge Nocedal and Stephen Wright. *Numerical optimization*. Springer Science & Business Media, 2006.
- [40] Cosmin G. Petra, Olaf Schenk, and Mihai Anitescu. Real-time stochastic optimization of complex energy systems on high-performance computers. *IEEE Comput. Sci. Eng.*, 16(5):32–42, 2014.
- [41] Florian A. Potra and Stephen J. Wright. Interior-point methods. *J. Comput. Appl. Math.*, 124(1):281–302, 2000.
- [42] Rehfeldt et al. A massively parallel interior-point solver for LPs with generalized arrowhead structure, and applications to energy system models. *EJOR Eur. J. Oper. Res.*, 296(1):60–71, 2022.
- [43] Scholz et al. Speeding up energy system models - a best practice guide. Technical report, BEAM-ME project, 06 2020.
- [44] Tamás Terlaky. *Interior point methods of mathematical programming*, volume 5. Springer Science & Business Media, 2013.
- [45] Stephen Wright. Stability of augmented system factorizations in interior-point methods. *SIAM J. Matrix Anal. Appl.*, 18(1):191–222, 1997.
- [46] Stephen J. Wright. *Primal-dual interior-point methods*. SIAM, 1997.